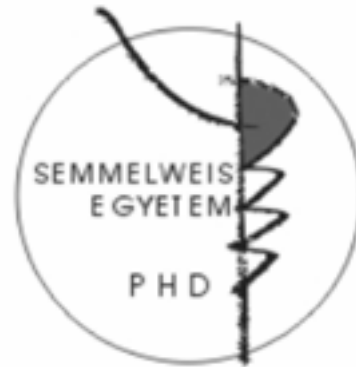


# First steps of tactile cortical processing in primates

Doctoral thesis

**Mária Ashaber**

Semmelweis University  
Szentágotthai János Doctoral School of Neuroscience



Supervisor: László Négyessy, PhD, senior research fellow

Opponents: Tamás Tompa, PhD, associate professor  
Viktória Vereczki, PhD, senior lecturer

President of examination board: Béla Víg, DSc, professor emeritus

Members of examination board: Zoltán Vidnyánszky, PhD full professor, DSc  
Attila Zsarnovszky, PhD, senior lecturer  
Árpád Dobolyi, PhD, senior research fellow

Budapest  
2014

## Content

1. Abbreviations .....	2
2. Introduction .....	3
3. Aims .....	4
4. Materials and methods .....	5
4.1 Animals .....	5
4.2 Surgery and histology .....	5
4.3 Identifying of target sites .....	5
4.4 Retrograde density maps .....	5
4.5 Laminar distribution: calculating SLN and SLP .....	6
4.6 Cortical magnification factor (CMF) .....	6
4.7 Electron microscopy .....	6
5. Results .....	6
5.1 Bidirectional tracing with BDA .....	6
5.2 Distribution of retrograde and anterograde labeling .....	7
5.3 Intra- and interareal connections .....	7
5.4 Quantitative analyses .....	7
5.4.1 Laminar distribution of retrograde and anterograde labeling .....	7
5.4.2 Cortical magnification factor (CMF) .....	7
5.4.3 Modularity .....	8
5.4.4 Synaptic organization .....	8
6. Conclusions .....	9
6.1 Importance of terminal axonal arborizations .....	9
6.2 Reciprocity of Br3b and Br1 connections .....	9
6.3 Connectivity of Br3b and Br1 .....	9

6.4	Anatomical correlates of somatosensory cortical hierarchy .....	10
6.4.1	Laminar distribution .....	10
6.4.2	Cortical magnification factor .....	10
6.4.3	Modular organization .....	10
6.4.4	Synaptic organization .....	10
6.5	New views of functional integration in the hand representations.....	11
6.6	Functional implications.....	11
6.6.1	Motion processing circuitry in postcentral somatosensory cortex .....	11
6.6.2	Braille reading .....	12
7.	Publication list.....	12
7.1	Publications used in dissertation.....	12
7.2	Other publications.....	13

## 1. Abbreviations

Br3a	Brodmann area 3a
Br3b	Brodmann area 3b
BDA	Biotinilated dextrane amine
CMF	Cortical magnification factor
DAB	1'3'-diamino-benzidin
NiDAB	Nikkel-intensified 1'3'-diamino-benzidine
IOS	Intrinsic signal optical imaging
RA	Rapidly adapting
PS	Postcentral somatosensory cortex
SAI	Slowly adapting

## 2. Introduction

Tactile perception plays important role in the exploration of the environment. However the functional tactile cortical processing underlying local connections are not known. The hand, especially distal fingertips play a fundamental role in touch and manual functions including haptic exploration. Postcentral somatosensory cortical (PS) Brodmann areas 3b (Br3b) and 1 (Br1) represent the first stages of cortical processing of tactile information (e.g. pressure, texture, shape), acquired via skin mechanoreceptors in primates (Sur et al., 1980; Iwamura, 1998). There are separate somatotopic maps in both areas, which are mirror symmetric to the Br1/Br3b boundary. There is an overrepresentation of the digit tips relative to other body parts, signifying that the two areas play an important role in touch. Connections of Br3b and Br1 are topographically organized, reciprocal and form patches (Burton and Fabri, 1995; Manger et al, 1997).

Br1 is thought as a higher level processing stage than Br3b (Sur et al., 1980; Iwamura 1998). Receptive fields of Br3b are small restricted to one finger, contrary receptive fields of Br1 cover more than one digits (Mountcastle and Powell, 1959; Hyvarinen and Poranen, 1978; Costanzo and Gardner, 1980; Sur et al., 1980, 1982, 1985; Iwamura et al., 1983a, 1993; Sripathi et al., 2006; Hsiao, 2008). The larger receptive fields in Br1 is thought as the result of more extensive intra- and interdigital integration (Iwamura et al., 1983b, Sinclair and Burton, 1991; Iwamura, 1998; Sripathi et al., 2006; Bensmaia et al., 2008; Pei et al., 2010). However in Br1 smaller cortical field is activated by stimulation of the same skin surface, than in Br3b, according to the different cortical magnification factor (CMF) in the tow areas (Friedman et al., 2008). Further physiological support of the hierarchical relationship is that the receptive fields of Br1 neurons are more complex than those in Br3b. This complexity is shown by an increased selectivity for stimulus motion and direction, and constancies for certain stimulus features (Iwamura et al., 1983b, Sinclair and Burton, 1991; Iwamura, 1998; Sripathi et al., 2006; Bensmaia et al., 2008; Pei et al., 2010). The laminar distribution of neuronal cell bodies and terminal axon arborizations are different in feedforward and feedback connections (Rockland and Lund, 1983; Felleman and Van, Essen, 1991; Barone et al., 2000). Laminar distribution of connections are different in Br3b and Br1, also suggesting their hierarchical relationship (Felleman and Van Essen, 1991). Furthermore, thalamocortical investigations show that feedforward or ascending connections form large boutons,

whereas feedback or descending afferents have rather small terminals (Hoogland et al., 1991; Sherman et al., 2012).

In our study we explored the preference of the local and interareal neuronal connections on the functional somatotopic maps of Br3b and Br1. Not like the visual cortex the combination of optical imaging and neuroanatomical techniques as made here have not been done in the primate's postcentral somatosensory cortex. In addition we investigate the synaptic organization of intra- and interareal connections to better understand the interaction of Br3b and Br1. Our results could help to understand processing of sensory processing, especially integration of digit tip representations. These studies could broaden our knowledge about structure- and function relationship in the somatosensory cortex, which could help robotic applications of haptic functions.

### **3. Aims**

1. To determine the connectional underpinning of the early steps of tactile perception we identified intra- and interareal input and target sites of the connections of distal finger pad representations by bidirectional tract tracing and functional mapping in Br3b and Br1 in the squirrel monkey. Preferred target areas, where synaptic integration plays significant role, were identified as regions with high density of axon terminal-like structures.
2. The morphological correlates of hierarchical relationship between Br3b and Br1 were examined by comparing relevant structural characteristics as follows:
  - a) Modularity of connectional distributions of Br3b and Br1.
  - b) Feedforward and feedback connections were determined based on laminar distribution of retrograde and anterograde labeling. Furthermore the ratio of supragranular neurons (SLN) and terminal arborizations (SLP) were compared in the two areas.
  - c) The extent local connectivity was compared to cortical magnification factor in Br3b and Br1.
  - d) Laminar, regional and areal distributions of large terminal-like structures were determined and their quantitative characteristics (volume and surface of boutons, size and number of mitochondria and postsynaptic densities) studied based on their three dimensional structure.

## **4. Materials and methods**

### **4.1 *Animals***

The animals used in the experiments were squirrel monkeys (*Saimiri sciureus*) 600-800 g of weight, 2-9 year of age, males (Mc, Mo and PB) and females (J, M and V). Keeping and operation methods met the requirements of IACUC (Institutional Animal Care and Use Committee) and those of NIH (National Institutes of Health). The experiments were done in cooperation with the department of psychology of Vanderbilt University (Nashville, TN, USA).

### **4.2 *Surgery and histology***

Anesthesia of the animals was done with ketamine-hydrochloride (10 mg / kg). Anesthesia was sustained by isoflurane inhalation (0,9-1,3%). The bidirectional tracer (BDA) was injected into the representational fields of stimulated digit tips, localized by intrinsic optical imaging signal (IOS) and electrophysiological methods in 3-3 animals (Br3b and Br1 injections, respectively). After survival times of 10-20 days, the animals were perfused. The standard avidine-biotine complex (ABC) protocol was used to visualize BDA labeling with nickel intensified diaminobenzidin (NiDAB) as the chromogen. After the NiDAB reaction sections were osmicated, dehydrated, infiltrated with resin and flat embedded on coated glass slides. Mapping of the BDA labeling was made with NeuroLucida.

### **4.3 *Identifying of target sites***

Densities of axon terminal-like structures were measured in regions containing either terminal patches, tracks of long range axons, or selected regions lacking retrograde labeling or distinct anterograde labeling.

### **4.4 *Retrograde density maps***

Density measurements of the retrograde labeling of cell bodies were performed by way of a Voronoi tessellation. Voronoi areas are inversely related to the density of the BDA labeled neurons. To compare across cases, the two dimensional density plots were computed based on Voronoi tessellation. "Uptake zone" labeling around the core of the injection site,

that measured 250-300  $\mu\text{m}$  diameter, was omitted from the analyses, and the distance between the serial sections was ignored. Finally, density maps were prepared based on standard deviation.

#### ***4.5 Laminar distribution: calculating SLN and SLP***

Barone et al. (2000) introduced a parameter determining ratio of supragranular labeled neurons (SLN).

SLN= number of labeled neurons of 1.-4. layers/all labeled neurons

In the same way we determined ratio of supragranular labeled terminal patches.

SLP= number of labeled terminal patches of 1.-4. layers/all labeled terminal patches

#### ***4.6 Cortical magnification factor (CMF)***

CMF= *cortical area (mm<sup>2</sup>)/represented skin area (mm<sup>2</sup>)*

Cortical regions of high local connectional densities were outlined and their size measured on the neuronal density plots in case of injections of Br3b and Br1. Skin areas represented by the outlined regions were calculated by using published values of cortical magnification factor (Friedman és mtsai, 2008).

#### ***4.7 Electron microscopy***

After mapping the large bouton-like elements with Neurlucida, series of ultrathin sections were cut from the regions selected for electron microscopic examination together with adjacent smaller labeled boutons. Ultrastructural characteristics were identified by conventional criteria (Peters et al., 1991).

## **5. Results**

### ***5.1 Bidirectional tracing with BDA***

Inputs and targets of connections of the injected locus of Br3b and Br1 were labeled by retrograde and anterograde BDA transport, respectively. Labeled neuronal cell bodies representing the input are retrograde labeled. The most of labeled neurons were identified as pyramidal cells. Anterograde axonal labeling also revealed the fine branching pattern and the presence of axon terminal-like structures.

## ***5.2 Distribution of retrograde and anterograde labeling***

The Voronoi diagram affords a measure of the retrograde labeling density at the neuronal level. Although, away from the injection site labeling density dropped with distance, clusters of retrogradely labeled neurons appeared medially, laterally, rostrally as well as caudally to the most heavily labeled region within injected areas. In neighboring areas retrogradely labeled neurons formed focal dense clusters. The anterogradely labeled horizontal fibers project in two directions: medioateral and rostrocaudal. The terminal arborizations are distributed mediolaterally more homogenously in Br1, than in Br3b, where terminal pathes were clustered more strongly.

## ***5.3 Intra- and interareal connections***

The BDA injection sites consisted the highest density of retrograde labeling. High density input to the injected digit representation originated from neighboring finger representations of the same area. In contrast, dense input from the neighboring areas' homotop finger pad representations characterized the interareal connections.

The labeled efferents in Br3b and Br1 showed a patchy pattern and were localized to in the homotop representation of the injected loci (i.e. the same distal finger pad). The highest density regions of retrograde and anterograde labeling distributed local in neighbor digit tip representations. In summary, the connections of distal finger pad representation organized mediolaterally within the injected areas and mostly restricted to the homotop digit representations of the neighboring areas in a reciprocal manner.

## ***5.4 Quantitative analyses***

### **5.4.1 Laminar distribution of retrograde and anterograde labeling**

Most of the labeled neurons and terminal arborizations were localized to the supragranular layers both within and between Br3b and Br1. Ratio of supragranular neurons (SLN) and terminal patches (SLP) were calculated and compared in all cases. Neither SLN nor SLP differed significantly between the areas.

### **5.4.2 Cortical magnification factor (CMF)**

The cortical magnification factor (CMF) is a ratio of the cortical and represented body surface. The highest retrograde density regions are measured and their averages



were computed. The highest density occupied significantly larger area in Br3b, than Br1 (Br3b injection: in Br3b:  $0,86 \pm 0,08$ ; average and SD; in Br1:  $0,4 \pm 0,05$ ; in Br1 injection: in Br3b:  $1,26 \pm 0,6$ ; Br1:  $0,4 \pm 0,05$  t-test,  $p < 0.01$ ). The size of the skin areas represented by the measured cortical surface were calculated by the CMF. The represented skin surface area did not significantly differ in Br3b and Br1 (in Br3b:  $6.5 \pm 1.8$  mm<sup>2</sup>; average and SD; in Br1:  $5.3 \pm 2$  mm<sup>2</sup>; t-test,  $p >> 0.05$ ).

### **5.4.3 Modularity**

The smallest Voronoi areas representing the most of labeled retrograde neurons (2 and 3 SDs above average) plotted depending of distance from the injection site. The density of neurons is decreased away from injection site. In Br3b high number of Voronoi areas appeared about 2500  $\mu$ m far from injection site, which is lower than that of injection site. In Br1 decreasing of density is rather homogenous, than in Br3b.

### **5.4.4 Synaptic organization**

The supra- and infragranular ratio of large bouton-like structures in case of Br3b and Br1 was not significantly different. We reconstructed some of these large terminal-like structures in 3D using serial section electron microscopy both in Br3b and Br1. Intra- and interareal afferents were characterized on the basis of functionally relevant ultrastructural features and three dimensional structure. We determined the size of labeled terminals, the number and size of mitochondria and postsynaptic densities. The average volume and surface area of the large terminals were 8-10 times larger than in case of small boutons (average $\pm$ SD; small bouton surface:  $1,34 \pm 0,65$ , and volume:  $0,25 \pm 0,23$ ; large bouton surface:  $13,3 \pm 9,8$  and volume:  $4,02 \pm 3,7$ ; t-test,  $p < 0,05$ ). There were no significant difference between large and small boutons in regard to the number and size of postsynaptic densities and that of mitochondria. 3D reconstruction of large boutons revealed their complex morphology including surface intrusions and protrusions.

## **6. Conclusions**

Connectivity of distal finger pad representations have not been investigated by combined anatomical and functional methods. We used bidirectional tracing combined with optical imaging and electrophysiological mapping to explore the connectivity of distal finger pad representations relative to the somatotopic maps of Br3b and Br1.

### ***6.1 Importance of terminal axonal arborizations***

In our results the distribution of terminal axon arborizations form patches, which supports previous results (Krubitzer and Kaas, 1990; Lund et al, 1993; Manger et al, 1997). The terminal patches were similar size (200-350  $\mu\text{m}$ ) as functional domains published previously (Chen et al., 2001; Friedman et al., 2004). Among the outputs the bouton-like structures were in largest number in the terminal patches. Our analyses strengthen that terminal arborizations represent specific target areas of distal fingertip representations in the postcentral somatosensory cortex.

### ***6.2 Reciprocity of Br3b and Br1 connections***

Regions with highest density retrograde and anterograde labeling overlapped resulting in reciprocal connectivity in and between Br3b and Br1. Based on our results Br3b and Br1 formed contacts in reciprocal manner. The efficacy of stereognosis and tactile perception could be increased by this reciprocity.

### ***6.3 Connectivity of Br3b and Br1***

Local connections spread mediolaterally within the injected areas, into the neighboring finger representations. Lower density of labeling appeared in more distal non-neighbor fingertip representations. Interareal connections indicate anteroposterior distribution and localised in homotop fingertip representations.

Br3b forms connections with neighbor areas, especially with Br1. Interareal connections of Br3b localized to homotop finger representations.

A notable difference found after Br1 injections compared with that of Br3b injections is that on the retrograde density maps the peak densities were surrounded by a larger spread of medium-to-low-density regions. This pattern of cortical connectivity implies that within Br1 high density, digit-matched inputs from Br3b form the anatomical

basis of receptive field hotspots and the lower density flanking regions could provide convergent input from neighboring fingertip representation to form the multifinger receptive fields. Furthermore, the fingertip regions of Br1 are connected more strongly with the proximal parts of the injected finger representations than in Br3b, which is consistent with the physiological observations (Iwamura et al., 1983b).

## ***6.4 Anatomical correlates of somatosensory cortical hierarchy***

### **6.4.1 Laminar distribution**

Mapping of feedforward and feedback connections could aid in investigating hierarchy in the cortex (Felleman and Van Essen, 1991). In our study labeled neurons and terminal arborizations are dominated in supragranular layers. These results suggest the lateral connectivity between Br3b and Br1 and feedforward connectivity from Br3b to Br1, respectively.

### **6.4.2 Cortical magnification factor**

The convergence will be increasingly more expressed in higher order cortical areas. In our results it appears that input from a similar surface area of the distal finger pads is processed by a significantly smaller amount of cortical tissue in Br1 than in Br3b (Friedman és mtsai, 2008). The larger convergence from the peripheral input in Br1 could be responsible for the more complex receptive field properties of this area compared to that of Br3b.

### **6.4.3 Modular organization**

Finger pad regions are represented less modular in Br1 than in Br3b (Iwamura et al., 1983). Our results support that connections of Br3b organized modular fashion (Sur et al., 1983).

### **6.4.4 Synaptic organization**

Anatomy of axonal terminals could determine neuronal network characteristics (feedforward or feedback), but synaptic features of corticocortical connections is less known. In thalamocortical connections, large terminals contribute feedforward connectivity (Van Horn és Sherman, 2004; Sherman és mtsai, 2012). Our

electronmicroscopic analysis shows that the identified big boutons have complex morphology, but interestingly they show similar properties in regard to other characteristics (sizes and number of mitochondria, postsynaptic densities).

## ***6.5 New views of functional integration in the hand representations***

The prevailing view of Br3b organization is that the response properties of cells are relatively simple, with receptive fields confined to single digits (e.g. Sur et al., 1985; DiCarlo et al., 1998). Contrary to this idea, recent electrophysiological studies reveal significant inter-digit integration across fingers within Br3b (Reed et al., 2008, 2010a,b; Lipton et al., 2010). These findings indicate that integration of cross-digit tactile information begins as early as Br3b. We suggest that intra-areal connections in Br3b play prominently in shaping multi-digit representation of global features of tactile objects, transfer of tactile aftereffects between fingers (Kappers, 2011), and in multifinger tasks and haptic exploration (Dijkerman and de Haan, 2007).

Based on the evidence that Br1 receives the bulk of its ascending input from Br3b (Shanks and Powell, 1981; Jones, 1983) and that ablation of Br3b silences Br1 (Garraghty et al., 1990), traditional views have suggested a hierarchical relationship between Br3b and Br1 (e.g. Powell and Mountcastle 1959; Sur et al., 1985). In contrast to small receptive fields in Br3b, Br1 neurons integrate information over larger skin areas and have higher order response properties such as preference for texture, roughness, or motion (Bensmaia et al., 2008; Pei et al., 2010; Tremblay et al., 1996). Accordingly, it is assumed that convergence of afferents of Br1 originating from Br3b is responsible for the observed somatosensory cortical hierarchy (Iwamura, 1998), but intraareal connections of Br1 expanded to more proximal parts of fingers.

## ***6.6 Functional implications***

### **6.6.1 Motion processing circuitry in postcentral somatosensory cortex**

Within Br1 neuronal responses are invariant to the specific cues contributing to the perception of motion supporting the view that it is a „motion processing” area and consistent with the predominance of cells with RA responses (Pei et al., 2010). In contrast, neurons selective for orientation tend to be slowly adapting (SA), a response type more common in Br3b than Br1 (Bensmaia et al., 2008). The findings of this study further refine this view by heavily restricting the interaction between Br3b and Br1 to homologous digit tip

representations, or potentially more generally to homologous skin representations. Thus, in contrast to the multi-digit integration present in Br3b and Br1, the functional transformations between Br3b and Br1 in the hand region are more fingertip-specific.

### **6.6.2 Braille reading**

There are many studies on the use dependent plasticity of the somatosensory cortical representation (for reviews see Jones et al., 2000; Godde et al., 2003; Wolters et al., 2005; Fox et al., 2009). In one example, blind subjects that use a single finger to read Braille have an expanded somatosensory cortical representation of that finger (Sathian and Stilla, 2010). Alternatively, the use of multiple fingers to read Braille can result in a disordered cortical representation accompanied by a reduced ability to localize finger stimulation (Sterr et al., 1998). Our findings suggest that existing intra-areal connectivity of Br3b provides at least in part a neuroanatomical locus of such use dependent plasticity. Most notably, in multiple-finger Braille readers a strengthening in the connectivity between the finger representations of Br3b could account for the decline in spatial discrimination.

## **7. Publication list**

### ***7.1 Publications used in dissertation***

**Ashaber** M, Pálfi E, Friedman RM, Palmer C, Jákli B, Chen LM, Kántor O, Roe AW, Négyessy L. (2014) Connectivity of somatosensory cortical area 1 form an anatomical substrate for the emergence of multifinger receptive fields and complex feature selectivity in the squirrel monkey (*Saimiri sciureus*). *J Comp Neurol*, doi: 10.1002/cne.23499.  
PMID:24214200

Négyessy L, Pálfi E, **Ashaber** M, Palmer C, Jákli B, Friedman RM, Chen LM, Roe AW. (2013) Intrinsic horizontal connections process global tactile features in the primary somatosensory cortex: neuroanatomical evidence. *J Comp Neurol*, 521 (12):2798-817.  
doi: 10.1002/cne.23317.  
PMID:23436325

## 7.2 *Other publications*

Négyessy L, Xiao J, Kántor O, Kovács GG, Palkovits M, Dóczi TP, Renaud L, Baksa G, Glasz T, **Ashaber** M, Barone P, Fonta C. (2010) Layer-specific activity of tissue non-specific alkaline phosphatase in the human neocortex. *Neuroscience*; 172:406-18. doi: 10.1016/j.neuroscience.

PMID: 20977932

Mikics E, Tóth M, Varjú P, Gereben B, Liposits Z, **Ashaber** M, Halász J, Barna I, Farkas I, Haller J. (2008) Lasting changes in social behavior and amygdala function following traumatic experience induced by a single series of foot-shocks. *Psychoneuroendocrinology*, 33 (9):1198-210. doi: 10.1016/j.psyneuen.

PMID:18656313